

## AFM Calculated Parameters of Morphology Investigation of Spin Coated MZO (M = Al, Sn, Cd, Co) Layers

M. Benhaliliba<sup>1,\*</sup>, A. Tiburcio-Silver<sup>2</sup>, A. Avila-Garcia<sup>3</sup>

<sup>1</sup> Department of Material Technology, Physics Faculty, USTOMB University, BP1505 Oran, Algeria

<sup>2</sup> ITT-DIE, Apdo, Postal 20, Metepec 3, 52176 Estado de Mexico, Mexico

<sup>3</sup> Cinvestav-IPN, Dept. Ingeniería Eléctrica-SEES, Apdo. Postal 14-740, 07000 México, D.F., Mexico

(Received 17 August 2015; published online 10 December 2015)

This paper reports on the deposition and surface properties of the pure and doped zinc oxide layers produced by spin coating route. Pure and metallic (Al, Sn, Cd, Co) doped ZnO films are characterized by mean of atomic force microscopy (AFM). Based on atomic force microscope observation, some parameters such as grain size, height, orientation of angle and histogram are determined. The AFM scanned 2D and 3D-views permit us to discover the roughness, the average height and the skewness of clusters or grains.

**Keywords:** Spin coating, ZnO layer, Metallic dopant, Atomic force microscope, Grain size, Roughness, Histogram.

PACS numbers: 68.37.Ps, 68.35.Ct, 81.05.Cy

### 1. INTRODUCTION

Nanostructures of pure and metallic doped ZnO are largely investigated in the search for improved properties and new applications due to its remarkable optical and electric properties. Growth of such layers is made by many processes like spray pyrolysis, spin and dip coating [1-6]. In this research, MZO (M = Al, Sn, Cd, Co) layers are fabricated by a facile and low cost spin coating technique. AFM details of morphology investigation of MZO (M = Al, Sn, Cd, Co) are explored, emphasized and calculated by the mean of 2D, 3D and histogram curves. In order to improve quality of topography of such nanostructures and their different properties and their use in micro and nano-electronic we fabricate such films.

### 2. PREPARATION AND ANALYSIS OF THE LAYERS

The ZnO layers have been grown by sol gel spin coating route onto glass slides  $76 \times 26$  mm substrate at speed of 1000 rpm. 0.5 Molar of dihydrated zinc acetate ( $\text{Zn}(\text{CH}_3\text{COO})_2 \cdot 2(\text{H}_2\text{O})$ ), (99.5 %) supplied by Carlo Erba reagents, is dissolved in 10 ml of 2-Methoxyethanol stirred at 60 °C for 10 mn and then 0.3 ml of the mono-ethanolamine (MEA) as stabilizer is added drop by drop, the clear solution is then obtained, the stirring continued for 60 min. The surface morphology of samples is analyzed by atomic force microscope (AFM) observation using a Quesant Model 250 system having an ( $80 \mu\text{m} \times 80 \mu\text{m}$ ) head, in the wave mode in air. For the ( $3 \mu\text{m} \times 3 \mu\text{m}$ ) square images the resolution is ( $300 \times 300$ ) pixels at a fixed scan rate of 2 Hz. All analyses are performed with the WSXM system software.

### 3. DATA AND PARAMETERS DISCUSSION

The root mean square (RMS) is given by [7],

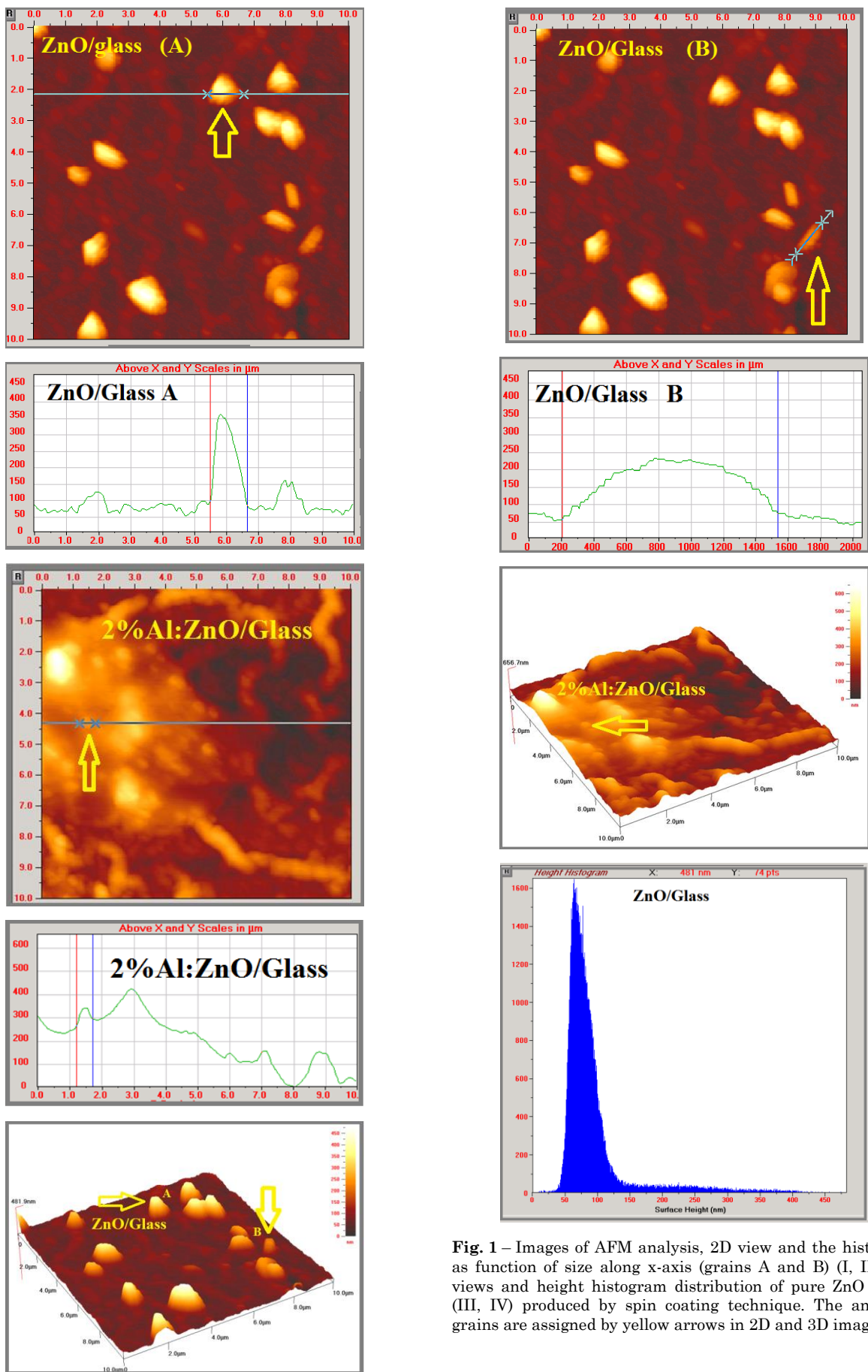
$$Rms = \sqrt{\frac{1}{N} \sum (Z_m - Z_i)^2} \quad (1)$$

Where  $N$  is the number of deviations,  $Z_i$  is the height reference and  $Z_m$  is the profile value. As tabulated below (Table 1), grain size, height, orientation angle and histogram parameters are determined using AFM observation and its suitable software. These analyses revealed the presence of assembled grains which have several orientations, shapes, roughnesses and sizes. The statistical distribution or height histogram showed a difference in intensity of bars (%), around 1600 for the ZnO case and 350 for the Cd (3 %) doped layer case.

The ZnO layer presents an average height of 93 nm a roughness (RMS) deviation of 56 nm as shown in Fig. 1 (height histogram). While the Al doped ZnO exhibits a height of 198.9 and 379 nm and RMS of 94 and 237 nm for 2 % and 3 % Al doping level respectively. Doped by cadmium, the layers present a height of 198 and 436 nm and RMS of 76 and 229 nm respectively for 2 and 3 % Cd doping level into solution as indicated in Table 1. The scanned AFM pictures showed a large amount of grain agglomeration that looked like assembled nanotips or nanocolumns with broadened heads and few voids as shown in Fig. 1. In 3D-shape, we observe the highest grain reached a value of 482 nm. The hollow ZnO nanocolumns have been fabricated by electrochemical deposition as reported by Cembrero [8]. The Figure 2 demonstrates the images of AFM analysis, 2D view and the histogram as function of size along x-axis. 3D-views and height histogram distribution of 2 % Al doped ZnO layers produced by spin coating technique are displayed in inset of the Figure 2.

The analyzed grains are assigned by yellow arrows in 2D and 3D images. The height histogram seems to be composed of many profiles where no symmetry occurs except the case of 2 and 3 % Sn and 2 % Cd doped ZnO films present a shape close to Gaussian distribution where a high symmetry of area height distribution is demonstrated. This result is confirmed by the homogeneity surface of sample which is easily seen in 3D-view (see Figures 4-6). It is reported in literature that AFM image shows hexagonally faceted columnar grains that dominate the surface morphology of (Al, B) co-doped ZnO by sol-gel process using spin coating procedure [9].

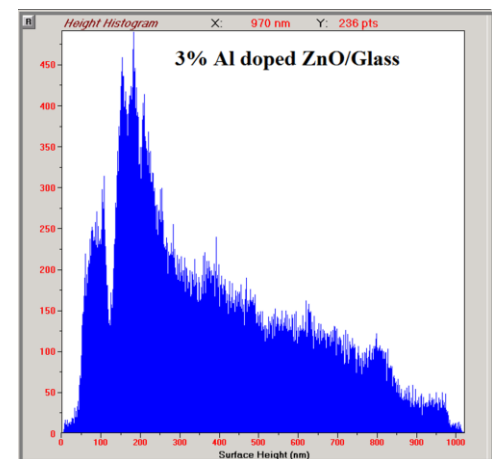
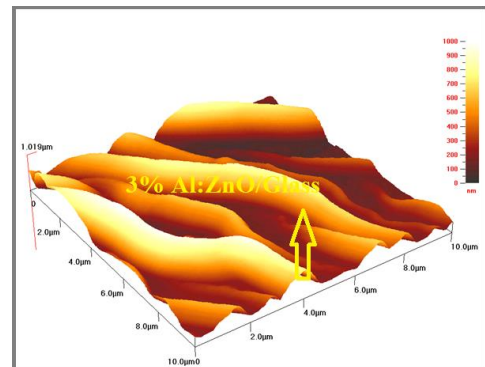
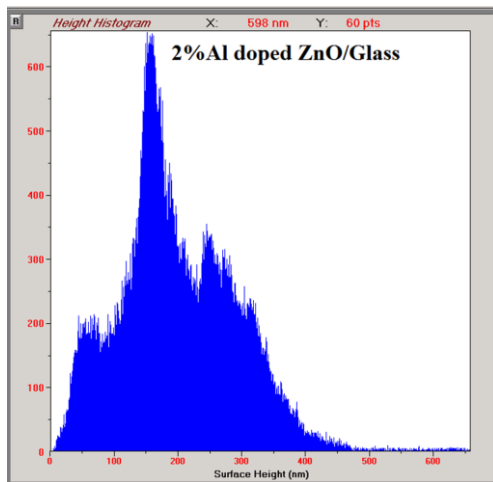
\* [mhenhaliliba@gmail.com](mailto:mhenhaliliba@gmail.com)



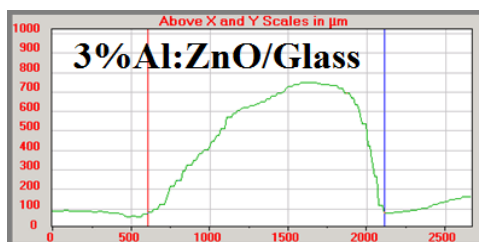
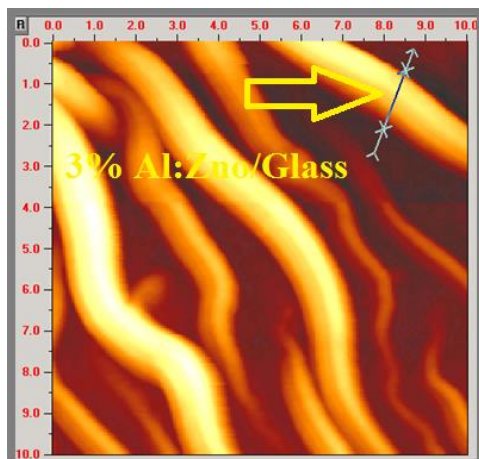
**Fig. 1** – Images of AFM analysis, 2D view and the histogram as function of size along x-axis (grains A and B) (I, II). 3D-views and height histogram distribution of pure ZnO layers (III, IV) produced by spin coating technique. The analyzed grains are assigned by yellow arrows in 2D and 3D images

**Table 1** – Description of the topography parameters of pure and M-doped ZnO produced by spin coating process @ 1000 rpm

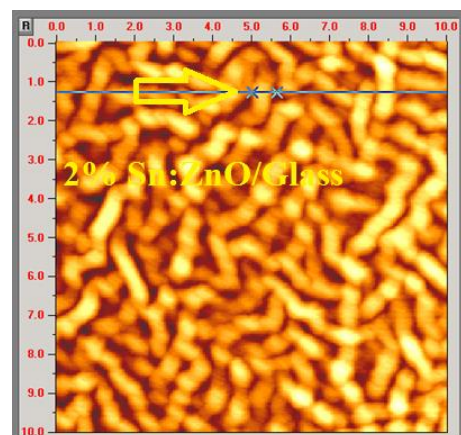
No	Material	Grain size (µm)	Height z (nm)	Orientation angle (°)	Histogram parameters	
					Average height (nm)	RMS deviation (nm)
1	Undoped ZnO/Glass (grain A)	1.16	7.17	89.6	93.10	59
2	Undoped ZnO/Glass (grain B)	0.84	17.52	89.2	93.1	59
3	2 % Al doped ZnO / Glass	0.51	28.6	86.8	198.8	94.17
4	3 % Al doped ZnO / Glass	0.54	6.38	89.8	378.7	237.2
5	2 % Sn doped ZnO / Glass	0.63	36.51	86.7	85.25	28.65
6	3 % Sn doped ZnO / Glass	0.51	0.50	89.9	124.3	41.9
7	2 % Cd doped ZnO / Glass	1.44	38.7	88.5	197.7	75.9
8	3 % Cd doped ZnO / Glas	1.35	42.3	88.2	435.7	228.6
9	Co doped ZnO / ITO	0.30	79.3	75.3	362	167.8

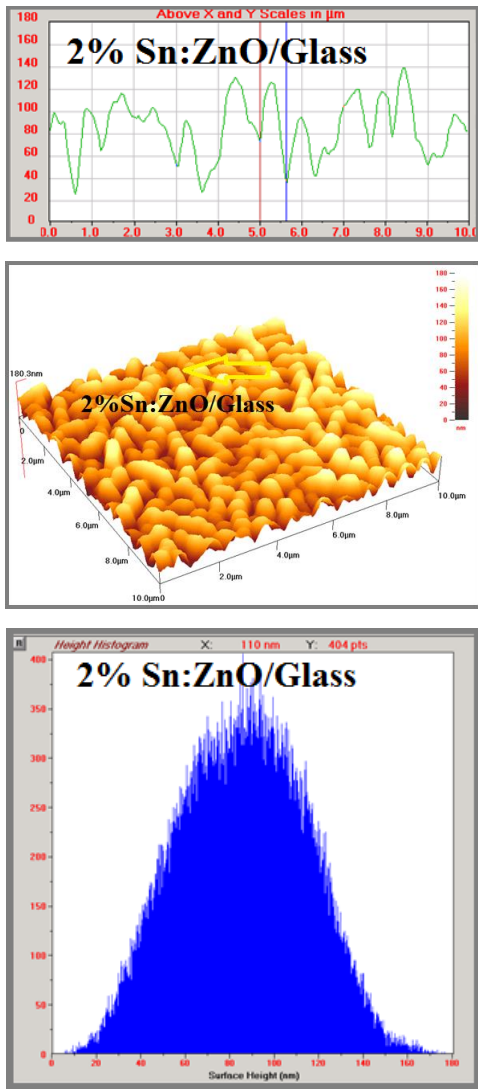


**Fig. 2** – Images of AFM analysis, 2D view and the histogram as function of size along x-axis. 3D-views and height histogram distribution of 2 % Al doped ZnO layers produced by spin coating technique. The analyzed grains are assigned by yellow arrows in 2D and 3D images

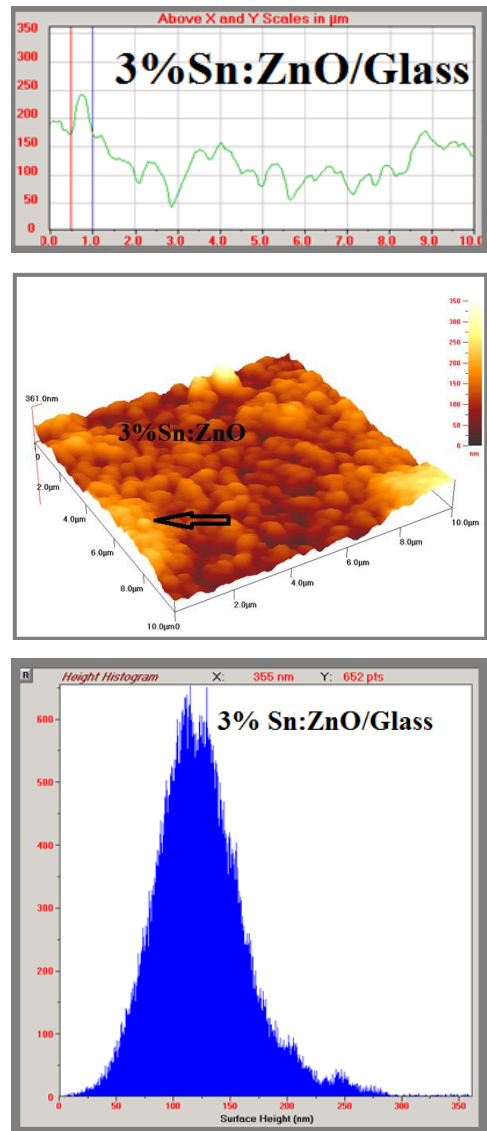


**Fig. 3** – Images of AFM analysis, 2D view and the histogram as function of size along x-axis. 3D-views and height histogram distribution of 3 % Al doped ZnO layers produced by spin coating technique. The analyzed grains are assigned by yellow arrows in 2D and 3D images

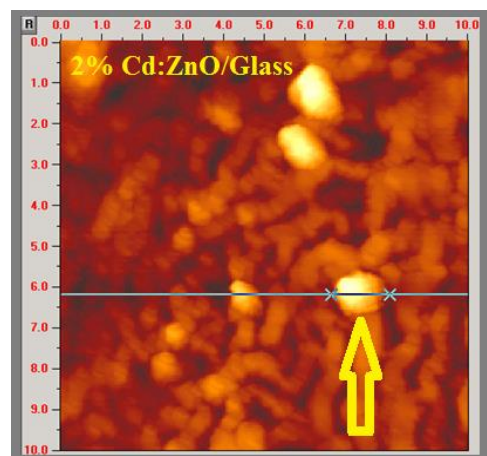
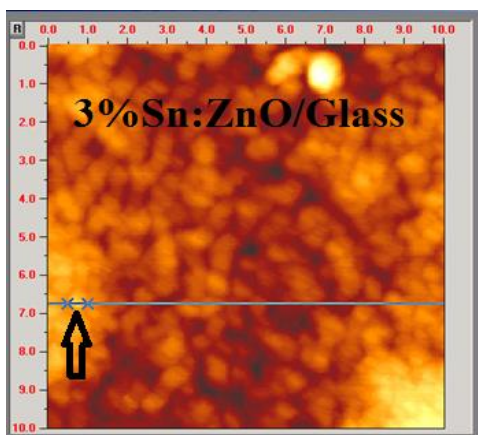




**Fig. 4** – AFM analysis pictures, 2D view and the histogram as function of size along x-axis. 3D-views and height histogram distribution of 2 % Sn doped ZnO layers produced by spin coating technique. The analyzed grains are assigned by yellow arrows in 2D and 3D images



**Fig. 5** – AFM analysis pictures, 2D view and the histogram as function of size along x-axis. 3D-views and height histogram distribution of 3 % Sn doped ZnO layers produced by spin coating technique. The analyzed grains are assigned by yellow arrows in 2D and 3D images



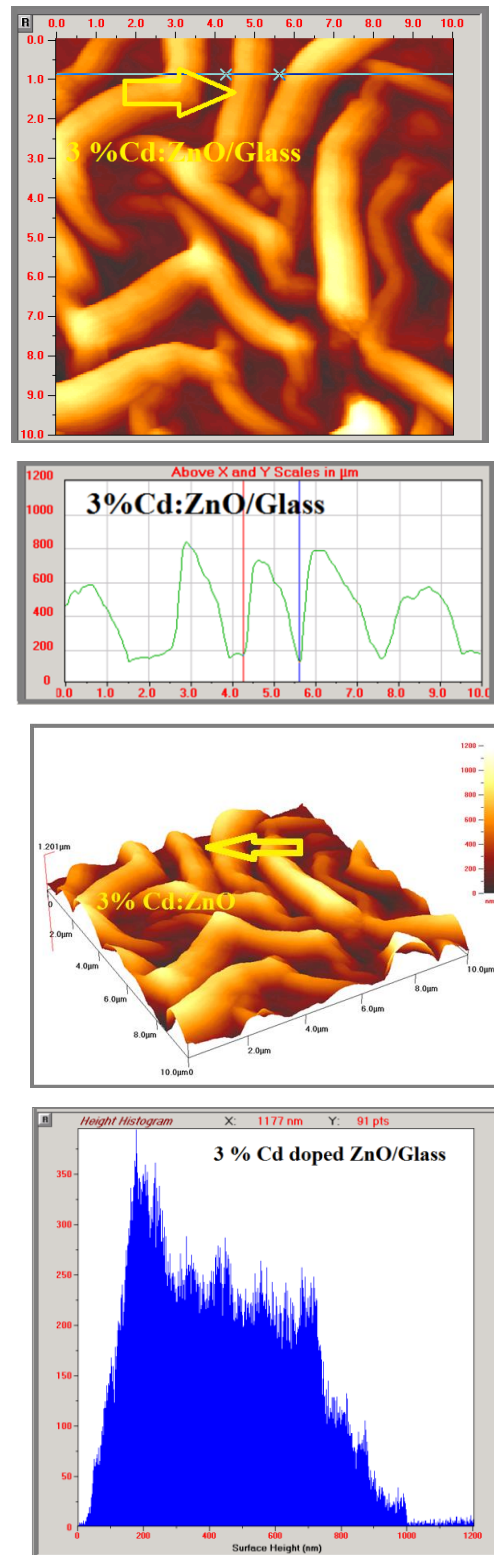
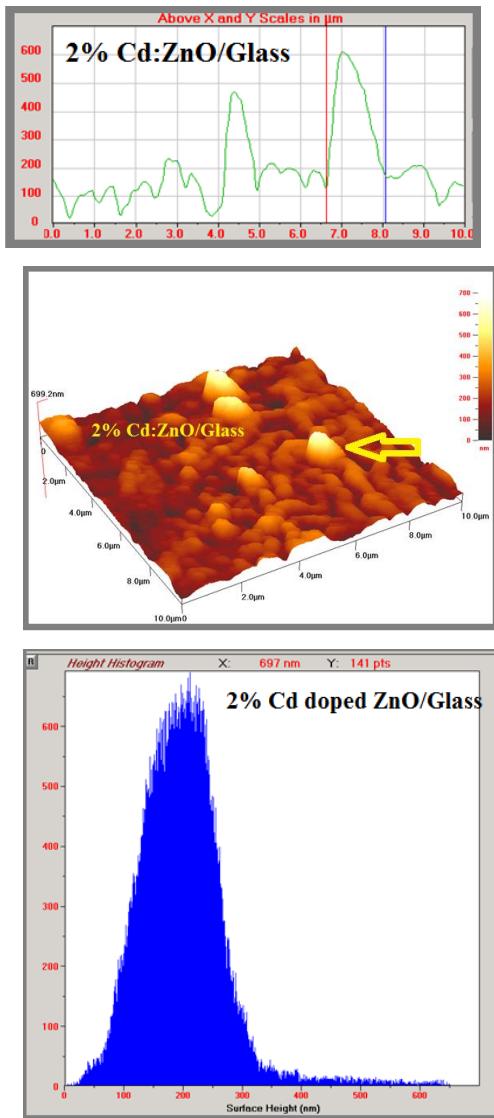


**Fig. 6** – The pictures of AFM analysis, 2D view and the histogram as function of size along x-axis. 3D-views and height histogram distribution of 2 % Cd doped ZnO layers produced by spin coating technique. The analyzed grains are assigned by yellow arrows in 2D and 3D images

The surface morphology of the ZnO film is practically smooth, with uniform grain distribution and the surface roughness was found to be 17 nm as cited by Sharma [10]. All our samples are roughly in well agreement with those found in literature.

The surface of as-grown ZnO layers, produced by spin coating technique, is composed by some non uniform domains. A topography of films was columnar as Smirnov mentioned in his work [14].

Furthermore, AFM images indicate that the ZnO films, deposited by sol gel spin coating, are formed from the nanoparticles as cited in literature [11] which corroborate with our results. Produced by a sol gel spin coating method @ 3000 rpm, the ZnO layers demonstrate the presence of a porous structure and the film surface for as-grown sample is very coarse with the root mean square (RMS) of 22.42 nm as Srinivasan reported [12] while our layers are more rough RMS > 40 nm. This fact might due to the minor speed (

**Fig. 7** – The images of AFM analysis, 2D view and the histogram as function of size along x-axis. 3D-views and height histogram distribution of 3 % Cd doped ZnO layers produced by spin coating technique. The analyzed grains are assigned by yellow arrows in 2D and 3D images

1000 rpm) of spin coating process used for the growth of our films. Moreover, the columnar character of the grains of pure and Fe-doped ZnO layer, prepared by spin coating at 3000 rpm, indicates the preferentially

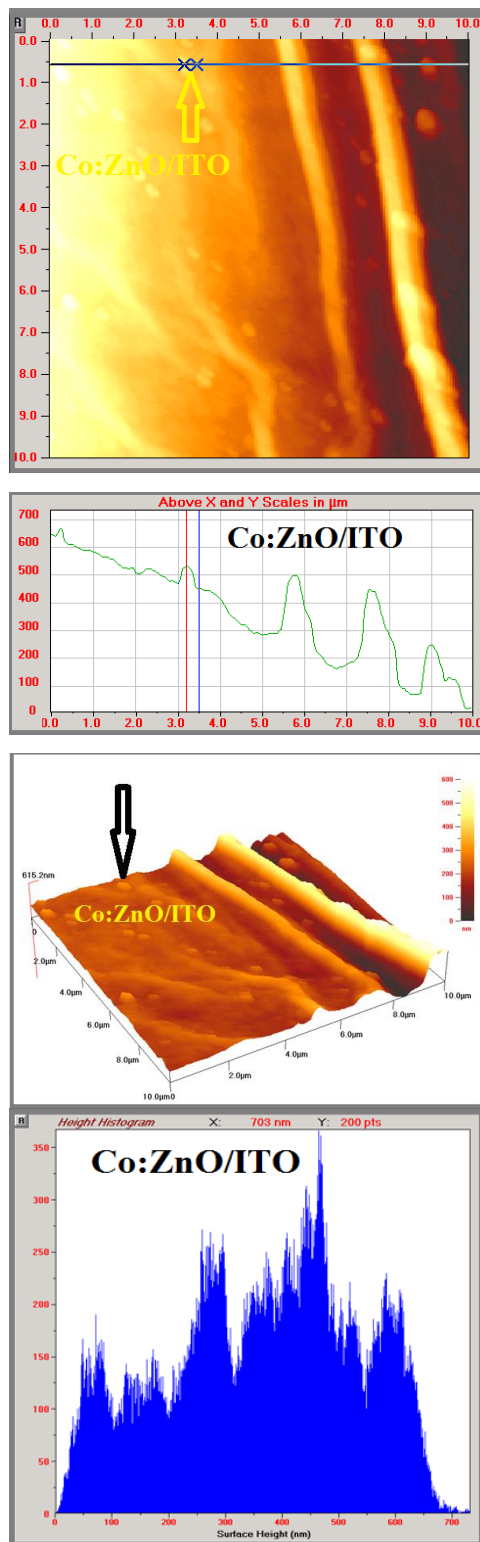


**Fig. 8** – The AFM analysis pictures, 2D view and the histogram as function of size along *x*-axis. 3D-views and height histogram distribution of Co doped ZnO layers produced by spin coating technique. The analyzed grains are assigned by yellow arrows in 2D and 3D images

growth along the *z*-axis direction perpendicular to the substrate surface as revealed by Rambu et al. [13].

The size of selected grains accurately showed by arrow in 2 and 3D views are determined by two vertical

red and blue lines inside of histogram as shown in figures. It is observed the formation of a crystalline film, with small grains ranging in micrometric size from 0.3-1.5  $\mu\text{m}$ , is observed as listed in table1 while the grain maximum height along *z*-axis is lesser < 80 nm. The orientation of grain relative to layer plane is nearly about 89° for the layers, 88° and 75° specially for cadmium and cobalt doped ones, which confirm the film growth along the *z*-axis as reported prior [2, 15]. The surface is lesser rough and RMS is of 59 for undoped sample and is higher for cobalt and aluminium doped ones as tabulated (Table 1).

The surface of 3%Al, 2%Sn and 3% Cd doped ZnO can be described as fibrous-type which might be a characteristic of an amorphous layer deposit as seen in figures 3, 4 and 7 in one hand. This trend was previously mentioned [2]. On the other hand, the 3% Sn: ZnO film shows a uniform texture which is formed by spheres as seen in 3D-view in figure 5 where the sizes are close, in the majority of the surface, evaluated at 0.5  $\mu\text{m}$  with a RMS roughness of 41.9 nm.

The Figures 6 and 7 depict the Cd doped ZnO layers in 2 and 3D configuration and histogram distribution. Cobalt doped ZnO film deposited on ITO substrate shows two long wrinkled range of grains as seen in Fig. 8. The grain size and RMS variation are plotted in double y-axis in Fig. 9.

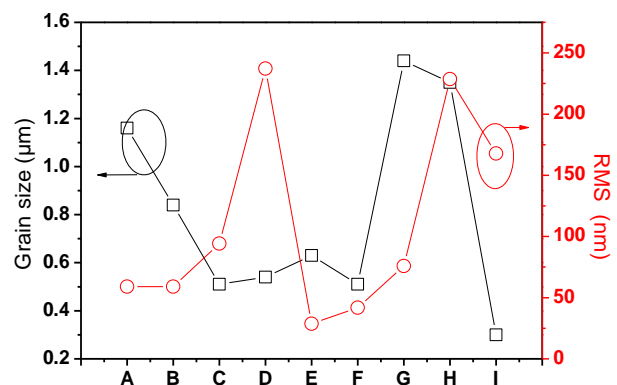


**Fig. 9** – Plotting of grain size (left) and RMS (right) deduced from AFM analysis (A: ZnO grain A, B: ZnO grain B, C: 2 % Al, D: 3 % Al, E: 2 % Sn, F: 3 % Sn, G: 2 % Cd, H: 3 % Cd, I:Co)-doped ZnO

#### 4. CONCLUSION

Prepared at 1000 rpm, nanostructure of pure and M-doped ZnO films are synthesized and explored by the AFM analysis. Many details are determined by the microscope observation and its suitable software. 2D-views show a non-homogenous surface with cluster and separated domains of grains. These latter have various shapes, sizes and roughnesses. Consequently, films more are rough  $240 > \text{RMS} > 40$  nm. The formed grain of layers are bigger, grain size are nano/micro metric (0.3-1.5  $\mu\text{m}$ ). Based on the angle orientation of the grown grains around 88°-89°, we confirm the growth of film along the *z*-axis. Such as-grown layers which exhibit nanostructured aspect could be utilized in micro and nanoelectronic devices and ferromagnetic systems for those doped with cobalt.

### ACKNOWLEDGEMENTS

The first author would like to acknowledge the head of virtual library SNDL <https://www.sndl.cerist.dz/>. This work was supported by ministry of high teaching and

scientific research [www.mesrs.dz](http://www.mesrs.dz) and Oran University of Sciences and technology [www.univ-usto.dz](http://www.univ-usto.dz). under CNEPRU (2013-2016) project N°B0L002UN31022-0130011.

### REFERENCES

1. M. Benhaliliba, A. Tiburcio-Silver, A. Avila-Garcia, A. Tavira, Y.S. Ocak, M.S. Aida, C.E. Benouis, *J. Semiconductor*. **36** No 8, 083001 (2015).
2. Mostefa Benhaliliba, *J. New Technol. Mater.* **4** No°1, 11 (2014).
3. M. Benhaliliba, C.E. Benouis, Z. Mouffak, Y.S. Ocak, A. Tiburcio-Silver, M.S. Aida, A.A. Garcia, A. Tavira, A. Sanchez Juarez, *Superlattice. Microstructure*. **63**, 228 (2013).
4. W. Chebil, A. Fouzri, A. Fargi, B. Azeza, Z. Zaaboub, V. Sallet, *Mat. Res. Bul.* **70**, 719 (2015).
5. Y. Aoun, B. Benhaoua, B. Gasmi, S. Benramache, *Optik* **126**, 5407 (2015).
6. Esam Al Arfaj, Ahmad Subahi, *Superlattice Microst.* **86**, 508 (2015).
7. A. Boukhachem, B. Ouni, M. Karyaoui, et al. *Mater. Sci. Semiconductor Proc.* **15**, 282 (2012).
8. J. Cembrero, D. Busquets-Mataix, E. Rayon, M. Pascual, M.A. Perez-Puig, B. Mari, *Mater. Sci. Semiconductor Proc.* **16**, 211 (2013).
9. Vinod Kumar, Neetu Singh, Avinashi Kapoor, Odireleng M. Ntwaeaborwa, Hendrik C. Swart, *Mater. Res. Bull.* **48**, 4596 (2013).
10. Bhupendra K. Sharma, Neeraj Khare, Shahzada Ahmad, *Solid State Commun.* **149**, 771 (2009).
11. Murat Soyly, Fahrettin Yakuphanoglu, *Mater. Chem. Phys.* **143**, 495 (2014).
12. G. Srinivasan, N. Gopalakrishnan, Y.S. Yu, R. Kesavamoorthy, J. Kumar, *Superlattice. Microstructure*. **43**, 112 (2008).
13. A.P. Rambu, C. Doroftei, L. Ursu, F. Iacomi, *Mater. Sci.* **48**, 4305 (2013).
14. M. Smirnov, C. Baban, G.I. Rusu, *Appl. Surf. Sci.* **256**, 2405 (2010).
15. M. Benhaliliba, C.E. Benouis, A. Tiburcio-Silver, Y.S. Ocak, *EPJ Web of Conferences* **44**, 03003 (2013).